

This is a repository copy of An experimental investigation of clearing effects in near-field and above-ground explosions.

White Rose Research Online URL for this paper: https://eprints.whiterose.ac.uk/id/eprint/233014/

Version: Accepted Version

Proceedings Paper:

Angelides, S., Bassam, B., Rigby, S. et al. (3 more authors) (2025) An experimental investigation of clearing effects in near-field and above-ground explosions. In: Proceedings of the 27th International Symposium on Military Aspects of Blast and Shock (MABS27). 27th International Symposium on Military Aspects of Blast and Shock (MABS27), 05-10 Oct 2025, Colmar, France. Military Aspects of Blast and Shock (MABS).

© 2025 MABS 27. For reuse permissions, please contact the Author(s).

Reuse

Items deposited in White Rose Research Online are protected by copyright, with all rights reserved unless indicated otherwise. They may be downloaded and/or printed for private study, or other acts as permitted by national copyright laws. The publisher or other rights holders may allow further reproduction and re-use of the full text version. This is indicated by the licence information on the White Rose Research Online record for the item.

Takedown

If you consider content in White Rose Research Online to be in breach of UK law, please notify us by emailing eprints@whiterose.ac.uk including the URL of the record and the reason for the withdrawal request.



AN EXPERIMENTAL INVESTIGATION OF CLEARING EFFECTS IN NEAR-FIELD AND ABOVE-GROUND EXPLOSIONS

Socrates C. Angelides¹, Bassam A. Burgan², Samuel E. Rigby³, Dain G Farrimond^{3,4}, Tommy Lodge^{3,4}, Andrew Tyas^{3,4}

¹Munitions Safety Information Analysis Center (MSIAC), NATO HQ, 1110
Brussels, Belgium;

²Steel Construction Institute, SCI, Unit 2, The E Centre, Bracknell, RG12
INF, UK;

³University of Sheffield, School of Mechanical, Aerospace and Civil
Engineering, Mappin Street, Sheffield, S1 3JD, UK;

⁴Blastech Ltd., The Innovation Centre, 217 Portobello, Sheffield, S1 4DP, UK

Key words: Blast Loading; Blast testing; Clearing; Near-field; Above-ground explosions.

ABSTRACT

When employing a risk management strategy for the storage of ammunition and explosives, as opposed to strictly adhering to established Quantity-Distances (QD), quantifying the effects of explosions is paramount. Practitioners, however, often face significant challenges in accurately predicting the resulting blast loading on Exposed Sites (ES). One major challenge lies in addressing the diffraction of the blast waves around the free edges of the impinged surface of the ES, which generates a pressure relief wave, thereby diminishing the reflected impulse. This phenomenon is known as blast wave clearing. The Hudson method, developed in 1955, is a first-principles approach to account for clearing effects by deriving pressure relief waveforms using the Sommerfeld diffraction theory. This method has been extensively validated through mid- and far-field experiments with surface charge open-arena blast tests. Recent comparisons with computational fluid dynamics (CFD) analyses have demonstrated the potential for extending the Hudson method to near-field and above-ground explosions. The former requires adjusting the pressure relief wave speed, as opposed to considering the constant ambient sound speed. For the later, when a target is located above the triple-point-path, two pressure relief waveforms are considered, corresponding to the incident and the ground-reflected waves that arrive separately at the target. This paper will investigate experimentally the clearing effects in near-field and above-ground explosions, and explore the application of the Hudson method to these scenarios.

INTRODUCTION

Accurate prediction of blast loading on Exposed Sites (ES) presents considerable challenges for practitioners, particularly due to the complex interaction of blast waves with finite structural surfaces. A critical aspect of this complexity arises from the diffraction of blast waves around the free edges of the impacted surface, which induces pressure relief waves that diminish the reflected impulse. This phenomenon, referred to

as blast wave clearing, leads to a progressive reduction of the reflected pressures on finite targets, ultimately approaching the lower pressures characteristic of the free-field environment.

To address this, Hudson [1] introduced a first-principles methodology for estimating clearing effects. This approach involves superimposing the reflected pressure-time history associated with an idealised infinite surface onto pressure relief waveforms emanating from the edges of a finite target. Figure 1a illustrates the resulting composite pressure-time history observed on a finite structure subjected to a surface charge detonation. This figure also delineates the constituent waveforms used in the superposition: the complete reflected pressure-time history for an infinite surface and the clearing wave (i.e., the pressure relief waveform). Hudson derived the waveforms using the Sommerfeld diffraction theory and presented them graphically as a function of the non-dimensional parameter $\eta = x/\lambda$, where x denotes the distance from the target point to the nearest free edge, and λ represents the spatial length of the positive phase of the incident Friedlander pulse—computed as the integral of acoustic wave speed over the duration of the positive phase.

Following the declassification of Hudson's work in 1998, there has been renewed scientific interest in investigating the accuracy of the Hudson clearing method. The Hudson method has undergone extensive validation in the mid- and far-field regions through computational fluid dynamics (CFD) simulations and open-field blast experiments involving surface charges placed on the ground [2, 3, 4]. More recently, Nartu et al. [5] demonstrated that the accuracy of the Hudson method in the near-field can be enhanced by refining the clearing wave speed used to compute the spatial length of the positive phase of the incident Friedlander pulse. Rather than employing a constant clearing velocity equivalent to the ambient sound speed, Nartu et al. proposed a variable clearing speed dependent on scaled distance. This velocity was derived analytically from the reflected pressure-time history on an idealised infinite surface, incorporating thermodynamic principles, acoustic wave propagation, and kinematic relationships. For scaled distances Z > 2 m/kg^{1/3}, where $Z = R/W^{1/3}$, R is the standoff distance between the charge and the target, and W is the charge weight, the analytical expression for the variable clearing speed showed strong agreement with CFD predictions. Building on this, Angelides et al. [6] extended the applicability of the modified Hudson method to scaled distances as low as Z > 0.8 m/kg^{1/3}, which approximates the fireball radius and was adopted as the lower bound for evaluating near-field validity. This threshold is significant because Hudson's original graphical derivation of pressure relief waveforms assumed a Friedlander-type blast wave impinging perpendicularly on a finite surface. Within the fireball region, however, the reflected pressure-time history profile deviates from the idealised Friedlander, or approximated triangular forms, due to the influence of expanding detonation products—a deviation substantiated by both numerical simulations [7] and experimental observations [8]. Despite these advancements, experimental validation of the Hudson method's near-field predictions for Z > 0.8 m/kg^{1/3} remains outstanding.

In above-ground explosion scenarios, where the explosive charge is positioned at a vertical elevation (V_E) above the ground surface, the wave reflection behaviour around a target point is governed by two distinct regimes. These regimes are determined by the target's relative position with respect to the triple-point path— the collection of points along the normal distance from the charge to the target point, where the incident wave

intersects with its ground-reflected counterpart, as illustrated in Figure 2. When the target lies above this triple-point path, the incident and ground-reflected waves reach the target sequentially rather than simultaneously. This temporal separation is evident in the pressure-time history shown in Figure 1b, which exhibits two distinct positive pressure peaks corresponding to the arrival of each wavefront.

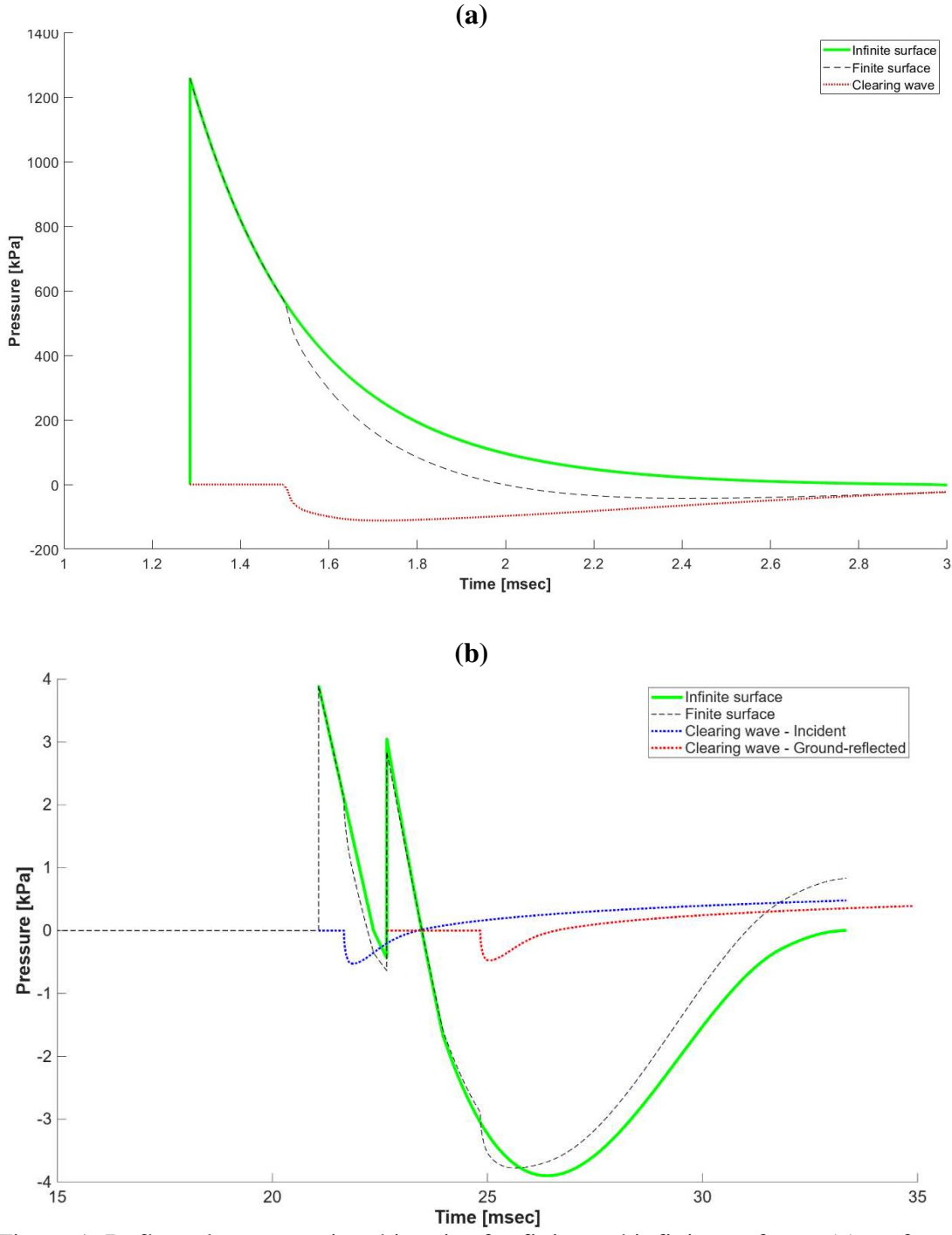


Figure 1: Reflected pressure-time histories for finite and infinite surfaces: (a) surface explosion or above-ground explosion with target located below the triple-point path, and (b) above-ground explosion with target located above the triple-point path.

Angelides et al. [6] examined the extension of the Hudson clearing method to finite surfaces where the target is positioned above the triple-point path. The analysis incorporated supplementary pressure relief waveforms that also account for the delayed arrival of the ground-reflected wave relative to the incident wave. The resulting composite pressure-time history for a finite structure subjected to an above-ground detonation is presented in Figure 1b. This figure also illustrates the individual components used in the superposition: the full reflected pressure-time history for an infinite surface, obtained via the EMBlast software [9] and the clearing waves (i.e., the pressure relief waveforms) derived from Hudson's graphical data. Notably, both clearing waves originate from the same free edge but propagate at distinct initiation times, corresponding respectively to the incident and ground-reflected wave arrivals. The modified Hudson method's predictions of positive phase impulse were evaluated against CFD simulations, showing good agreement. However, experimental validation of these above-ground explosion predictions has yet to be conducted.

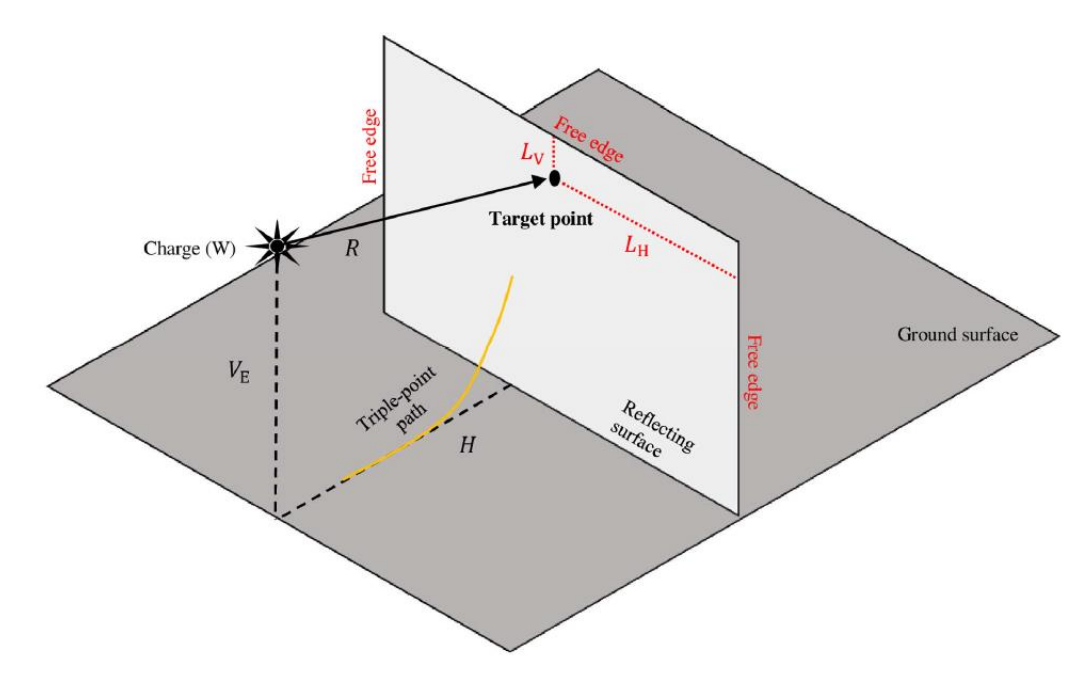


Figure 2: Sketch of an above-ground explosion with target located above the triple-point path [6].

This paper will present experimental blast trials aimed at investigating clearing effects and evaluating the applicability of the Hudson method in scenarios that, until now, have been examined exclusively through CFD simulations. The focus will be on aboveground explosions with targets located above the triple-point path and near-field blast loading.

EXPERIMENTAL METHOD

A total of 14 new experiments were performed at the University of Sheffield (UoS) Blast and Impact Laboratory in Buxton, UK. Each experiment involved the detonation of a single charge positioned between two identical vertical walls, each measuring 1.2

m in height (H) and 1.2 m in width (L). The test matrix comprised two distinct configurations based on the height of burst: surface charge detonations and above-ground detonations, as outlined in Tables 1 and 2, respectively, which detail the parameters of each experimental setup. Reflected pressure-time histories were captured using a total of 12 pressure gauges, with six gauges mounted on each wall. The spatial arrangement of these gauges is illustrated in Figure 3, where Figure 3a corresponds to the surface charge configuration and Figure 3b to the above-ground explosion setup.

Table 1: Near-field blast experimental program.

Test designation	Height of burst, $h_{\rm e}$ [m]	Charge type	Charge mass, W [g]	Standoff distance (Wall A), R _A [m]	Standoff distance (Wall B), R _B [m]
NF_A_1	0	PE10	115	1.2	1.2
NF_A_2	0	PE10	115	1.2	1.2
NF_A_3	0	PE10	115	1.2	1.2
NF_A_4	0	PE10	115	1.2	1.2
NF_A_5	0	PE10	115	1.2	1.2
NF_B_1	0	PE10	170	1.2	1.2
NF_B_2	0	PE10	170	1.2	1.2
NF_B_3	0	PE10	170	1.2	1.2

Table 2: Above-ground blast experimental program.

Test designation	Height of burst, he [m]	Charge type	Charge mass, W[g]	Standoff distance (Wall A), R _A [m]	Standoff distance (Wall B), R _B [m]
AG_A_1	0.4	PE10	8	1.2	1.2
AG_A_2	0.4	PE10	8	1.2	1.2
AG_A_3	0.4	PE10	8	1.2	1.2
AG_B_1	0.4	PE10	15	1.2	1.2
AG_B_2	0.4	PE10	15	1.2	1.2
AG_B_3	0.4	PE10	15	1.2	1.2

To facilitate the evaluation of clearing effects, both target walls in each test configuration were positioned equidistantly from the explosive charge, with standoff distances R_A and R_B set to 1.2 m. However, the alignment of the charge relative to the walls was intentionally varied. As illustrated in Figure 3, the charge was centred with respect to Wall B and gauges B1 and B2, which were located at the mid-span of the wall, corresponding to a horizontal distance of 0.6 meters from the free edge (i.e., L/2). In contrast, Wall A was laterally displaced, resulting in the charge being aligned with gauges A3 and A4, situated 0.2 m from the horizontal free edge. This configuration enables a direct comparative analysis of the reflected pressure-time histories recorded at B1 versus A3, and B2 versus A4. The instrumentation on Wall B represents conditions approximating an infinite target, where clearing effects are minimal, whereas Wall A simulates a finite target scenario, in which clearing effects are expected to be more pronounced.

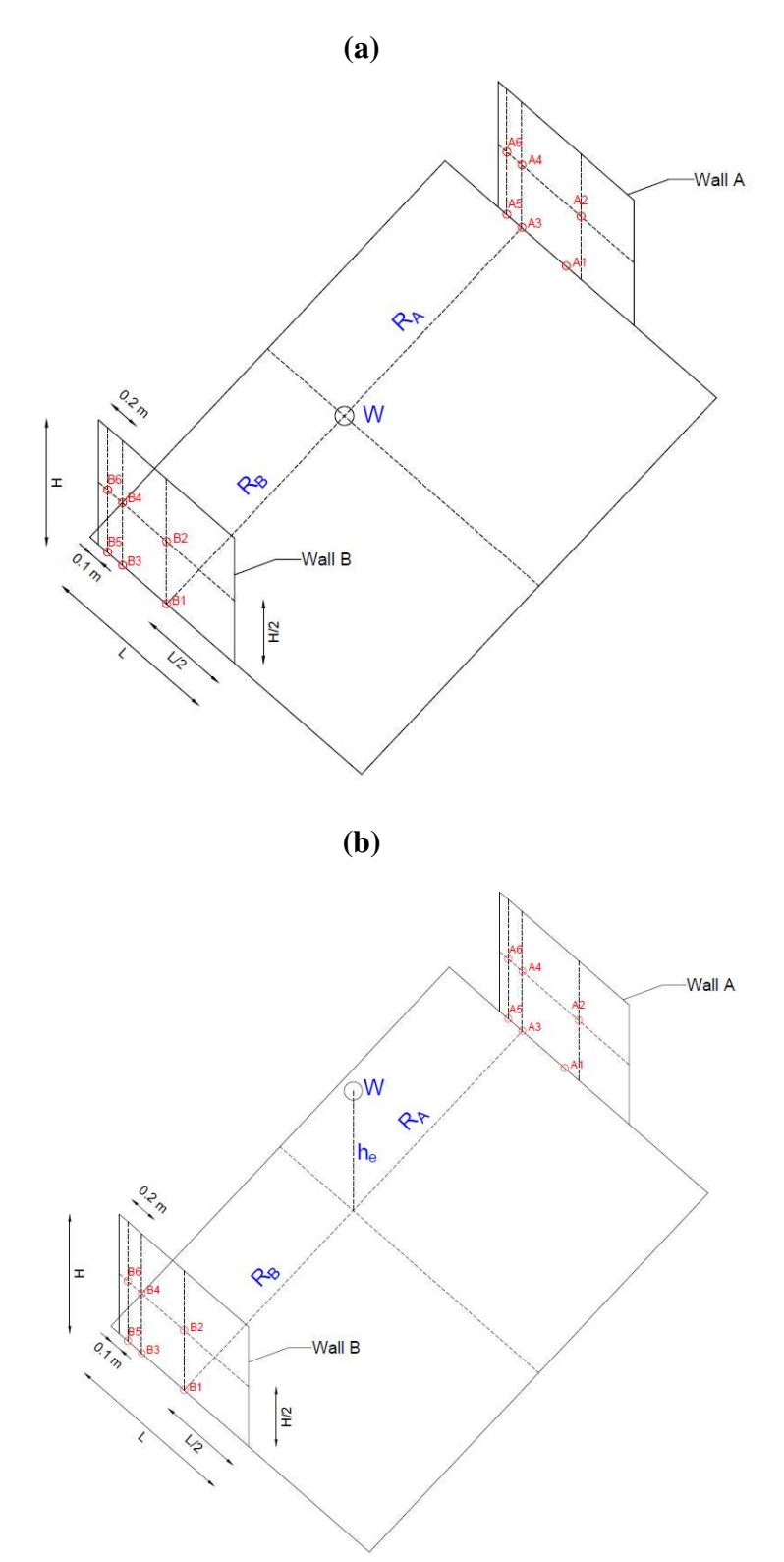


Figure 3: Sketches showing the experimental setup for the: (a) near-field surface blast tests and (b) above-ground blast tests. A1 to A6, and B1 to B6, designate the location of pressure gauges in Wall A and B, respectively. H and L are the heigh and width of the walls, W is the charge weight, R_A and R_B are the standoff distances to Wall A and B, respectively, and h_e is the height of burst.

The primary objective of the first test configuration, involving surface charge detonations, was to investigate near-field clearing effects. The experimental campaign employed PE10 explosive charges of two distinct masses: 115 g (Tests NF_A_1 to NF_A_5) and 170 g (Tests NF_B_1 to NF_B_3). These charge sizes were selected to assess clearing effects under near-field conditions. Applying a TNT equivalence factor of 1.22 [10], the corresponding scaled distances were calculated as Z = 2.31 m/kg^{1/3} and 2.03 m/kg^{1/3}, respectively. To ensure data reliability and repeatability, each test was conducted three times. However, the 115 g charge tests were repeated five times due to instrumentation failures and inconsistencies observed in the recorded data.

The second experimental configuration, which involved above-ground explosive detonations, was designed to examine clearing effects on targets situated above the triple-point path. To achieve this, gauge placements were strategically determined to capture data both below and above the triple-point path. Gauges positioned at ground level along the base of Walls A and B (A1, A3, A5, B1, B3, and B5) correspond to locations beneath the triple-point path, while those mounted at mid-height (H/2 = 0.6 m) on the walls (A2, A4, A6, B2, B4, and B6) represent positions above it. The test series utilised PE10 explosive charges of two different masses—8 g (Tests AG_A_1 to AG_A_3) and 15 g (Tests AG_B_1 to AG_B_3)—selected to isolate and evaluate clearing effects under mid-field conditions. This approach was intended to minimise the influence of near-field complexities and focus specifically on the dynamics of above-ground blast interactions. Again, using a TNT equivalence factor of 1.22, the scaled distances were computed as Z = 5.62 m/kg^{1/3} and 4.55 m/kg^{1/3}, respectively. Each test was repeated three times to ensure consistency and reliability of the measurements.

The applicability of the Hudson methodology to near-field and above-ground explosion scenarios was examined by comparing its predictions with results from the four distinct experimental tests. These predictions were generated using the EMBlast software [9], which applies the Low Altitude Multiple Burst (LAMB) rules to derive reflected pressure-time histories and the Hudson method to incorporate the influence of clearing effects.

RESULTS AND DISCUSSION

This section presents and examines the results obtained from blast experiments conducted under both near-field and above-ground detonation scenarios. The recorded data are then compared with the theoretical predictions provided by the Hudson method.

Near-field explosions

Figures 4 and 5 display the experimental data obtained from surface charge detonations conducted under near-field conditions. Figure 4 presents results from five repeated trials using a 115 g charge (Tests NF_A_1 to NF_A_5), while Figure 5 shows data from three repetitions with a 170 g charge (Tests NF_B_1 to NF_B_3). Both figures include reflected pressure-time histories and the corresponding reflected impulse-time histories derived from the measurements.

Subfigures 4a, 4c, 5a, and 5c focus on data from gauges A3, A5, and B1. This selection enables a direct comparison between gauges A3 and B1, which are both aligned with the explosive charge. Gauge A3 is positioned 200 mm from the horizontal free edge, whereas gauge B1 is centrally located on the wall, 600 mm from the edge. Gauge A5

is also included, positioned 100 mm further from A3 and thus 100 mm from the horizontal free edge, although it is not directly aligned with the charge.

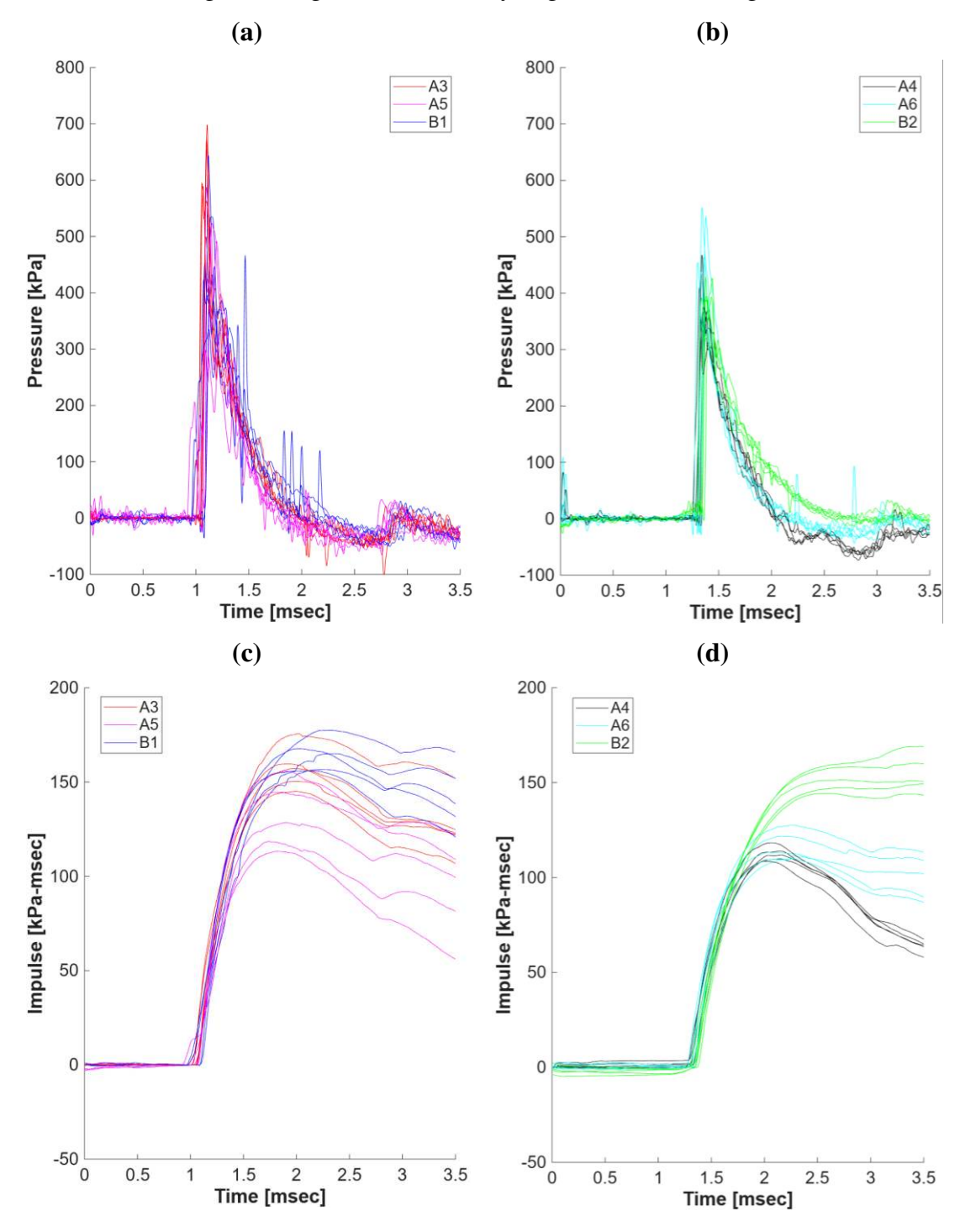


Figure 4: Near-field blast results for tests NF_A_1 to NF_A_5: (a) reflected pressure-time histories recorded at gauges A3, A5 and B1, (b) reflected pressure-time histories recorded at gauges A4, A6 and B2, (c) reflected impulse-time histories derived at gauges A3, A5 and B1 and (c) reflected impulse-time histories derived at gauges A4, A6 and B2.

Similarly, subfigures 4b, 4d, 5b, and 5d present measurements from gauges A4, A6, and B2. These gauges follow the same spatial logic as those in the previous subfigures but are all mounted at a vertical height of 600 mm above the charge. Consequently, the recorded data in these cases are influenced by variations in the angle of incidence.

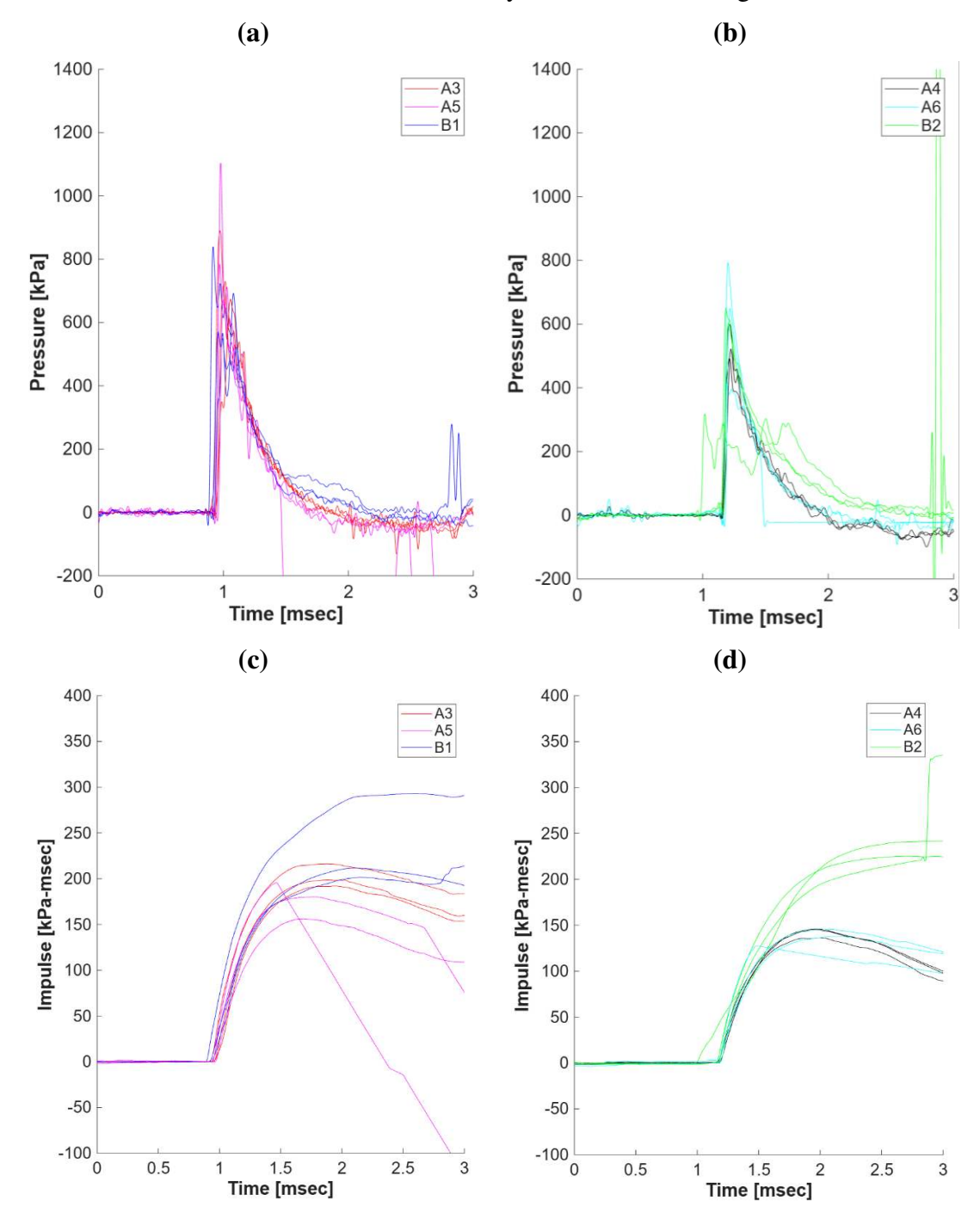


Figure 5: Near-field blast results for tests NF_B_1 to NF_B_3: (a) reflected pressure-time histories recorded at gauges A3, A5 and B1, (b) reflected pressure-time histories recorded at gauges A4, A6 and B2, (c) reflected impulse-time histories derived at gauges A3, A5 and B1 and (c) reflected impulse-time histories derived at gauges A4, A6 and B2.

Figures 4 and 5 demonstrate generally strong repeatability across the series of near-field blast tests, despite occasional gauge malfunctions attributed to the extreme pressures characteristic of the near-field regime. For both explosive charge masses, gauge B1 consistently recorded higher reflected pressure-time histories than gauges A3 and A5, as illustrated in Figures 4a and 5a. A similar trend is observed for the gauges located at a vertical elevation with respect to the charge, with gauge B2 recording higher reflected pressures than gauges A4 and A6, as depicted in Figures 4b and 5b. This becomes more pronounced in the corresponding reflected impulse-time histories shown in Figures 4c and 5c, (and 4d and 5d) offering compelling evidence that clearing effects remain significant in the near-field, even at scaled distances as low as 2 m/kg^{1/3}.

A comparative analysis of gauges A3 and A5—both situated near the horizontal free edge—shows that gauge A5 consistently records lower pressure values. This observation is consistent with its closer proximity to the free edge, where clearing effects are expected to be more pronounced. Nonetheless, the reduced pressure at A5 may also be partially attributed to angle of incidence effects, as it is not directly aligned with the explosive charge. In contrast, a similar trend is not observed for gauges A4 and A6; in most cases, gauge A6 registers higher pressures despite being positioned nearer to the free edge, where lower values would typically be anticipated due to clearing. This discrepancy suggests that angle of incidence may play a more significant role in these measurements. Future investigations will aim to better understand how angle of incidence and clearing effects jointly affect pressure measurements in the near-field.

Above-ground explosions

Figures 6 and 7 illustrate the results collected from the above-ground blast experiments. Figure 6 contains data from three repeated tests conducted with an 8 g charge (Tests AG_A_1 to AG_A_3), whereas Figure 7 presents outcomes from three trials using a 15 g charge (Tests AG_B_1 to AG_B_3). Each figure features both the reflected pressure-time histories and the associated reflected impulse-time histories obtained from the recorded measurements.

Figures 6 and 7 show consistent repeatability across the above-ground blast trials. In Figures 6a and 7a, gauges A4, A6, and B2—positioned at a height of 0.6 m above ground level and thus above the triple-point path—exhibit two distinct positive pressure peaks. This pattern confirms that the incident and ground-reflected waves arrive at these locations in sequence rather than simultaneously, as outlined in Section 1. In contrast, gauges A3, A5, and B1, located at ground level and therefore below the triple-point path, display a single positive peak, which aligns with expectations. These ground-level gauges also record significantly higher peak pressures compared to those above the triple-point path, due to the combined impact of the incident and reflected waves forming a Mach stem at these positions.

The pressure-time histories shown in Figures 6a and 7a clearly indicate that clearing effects influence targets positioned both below and above the triple-point path. For targets below the triple-point path, gauge B1 consistently measured higher reflected pressures than gauges A3 and A5. Likewise, for targets above the triple-point path, gauge B2 recorded higher reflected pressures compared to gauges A4 and A6. This trend becomes even more apparent in the reflected impulse-time histories illustrated in

Figures 6b and 7b, and was consistently observed across both explosive charge sizes used in the tests.

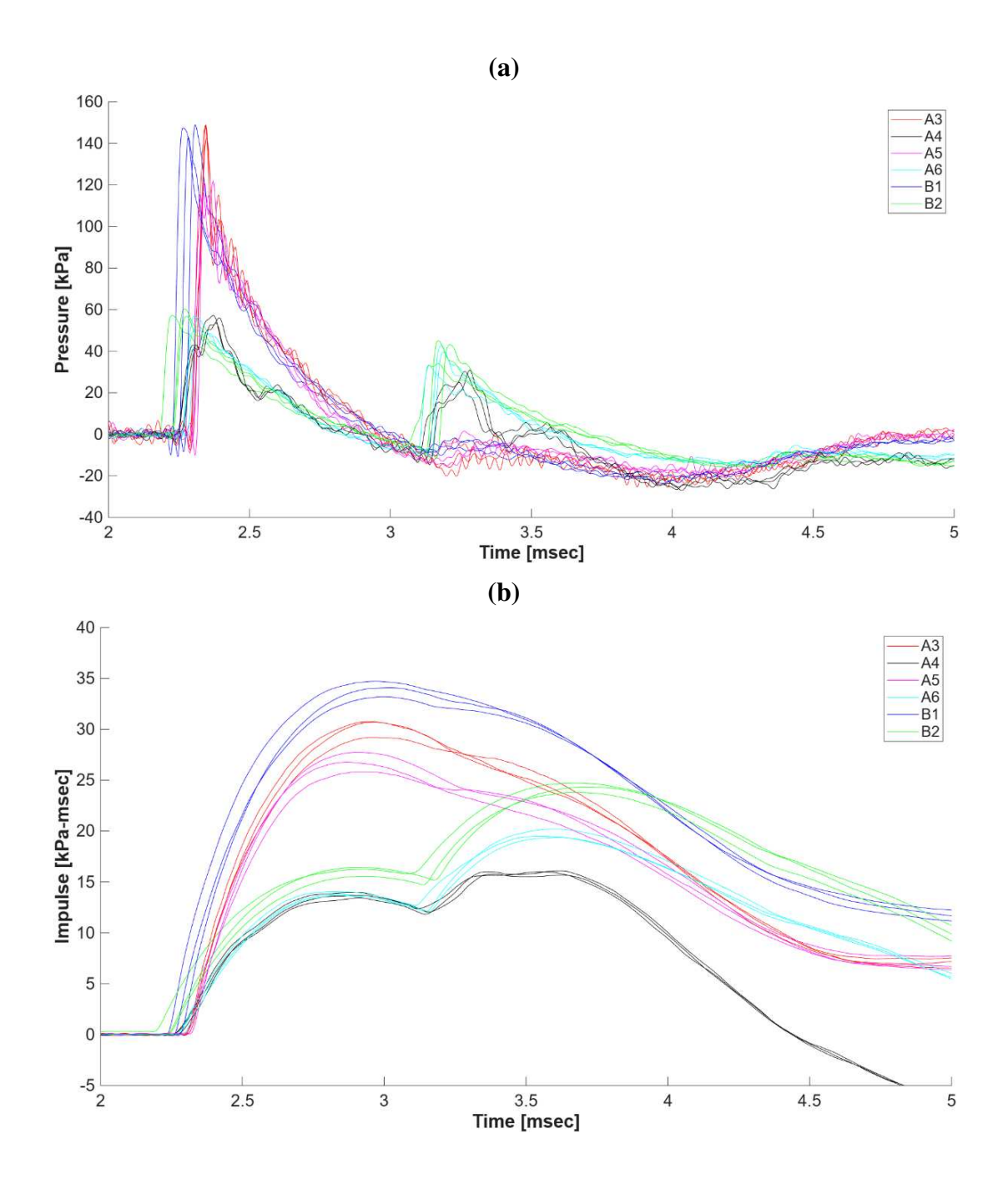


Figure 6: Above-ground blast results for tests AG_A_1 to AG_A_3: (a) reflected pressure-time histories recorded at gauges A3, A4, A5, A6, B1 and B2, and (b) reflected impulse-time histories derived at gauges A3, A4, A5, A6, B1 and B2.

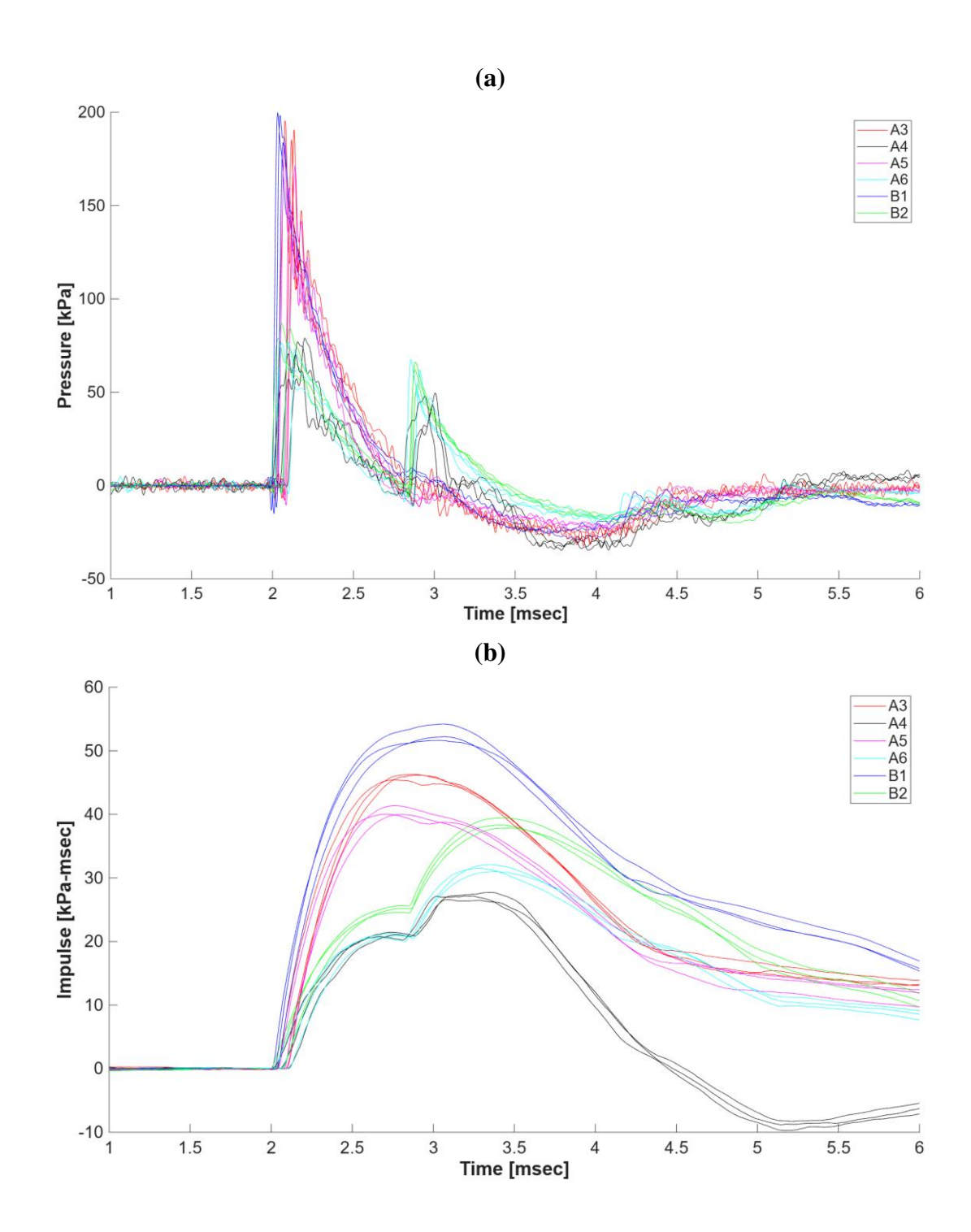


Figure 7: Above-ground blast results for tests AG_A_1 to AG_A_3: (a) reflected pressure-time histories recorded at gauges A3, A4, A5, A6, B1 and B2, and (b) reflected impulse-time histories derived at gauges A3, A4, A5, A6, B1 and B2.

Assessment of the Hudson method in the near-field and above-ground explosions

To evaluate the theoretical predictions of the Hudson method for both near-field and above-ground explosions, the experimental data are compared with simulations generated by the EMBlast software, which integrates the Hudson method to account for

clearing effects. For clarity and to avoid redundancy from repeated trials, only one representative test result is presented for each case. In the near-field explosion tests, data from gauges A3 and B1 are used exclusively, as these gauges are directly aligned with the explosive charge and thus unaffected by variations in the angle of incidence. Likewise, for the above-ground tests, only readings from gauges A4 and B2 are considered.

Figures 8 and 9 depict the comparative analysis for near-field explosion scenarios, corresponding to charge masses of 115 g and 170 g, respectively. The LAMB rules demonstrate strong agreement with the experimentally measured reflected pressuretime histories on an idealised infinite surface (gauge B1). Specifically, the model predicts peak reflected pressures of 677 kPa and 1002 kPa for the 115 g and 170 g detonations, respectively, compared to measured values of 644 kPa and 717 kPa. The observed underestimation in recorded peak pressures for the 170 g trial is likely attributable to the limitations of the gauges in capturing extreme near-field overpressures. Arrival times of the pressure waves were consistent between the LAMB rules and experimental data, both occurring around 1.1 msec. Additionally, the Hudson method forecasts the onset of clearing at approximately 1.6 msec for both scenarios, which aligns with experimental observations—specifically, a drop in pressure recorded by gauge A3 relative to gauge B1 at that moment. These initial experimental findings reinforce earlier CFD simulation results, indicating that the Hudson method effectively predicts clearing effects in near-field conditions, even at scaled distances as small as 2 $m/kg^{1/3}$.

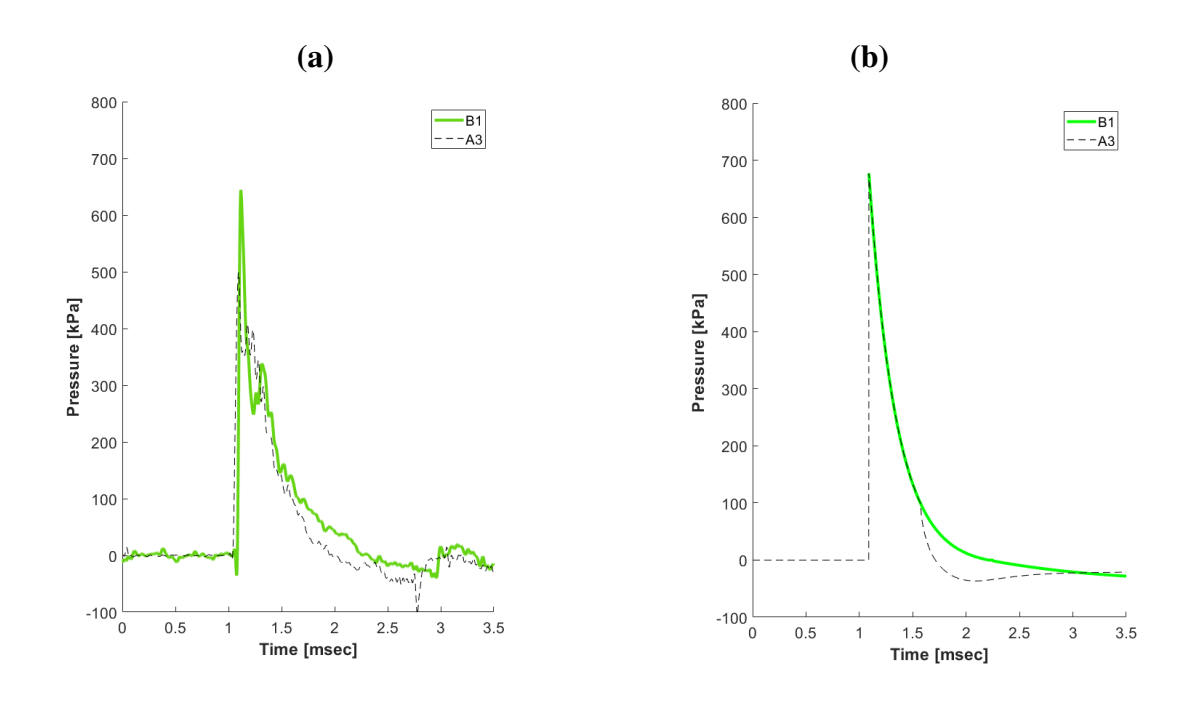


Figure 8: Assessment of clearing effects in the near-field for 115 g detonation: (a) pressure-time histories recorded from blast trials at gauges A3 and B1 in test NF_A_3, (b) pressure-time histories predicted with the Hudson method.

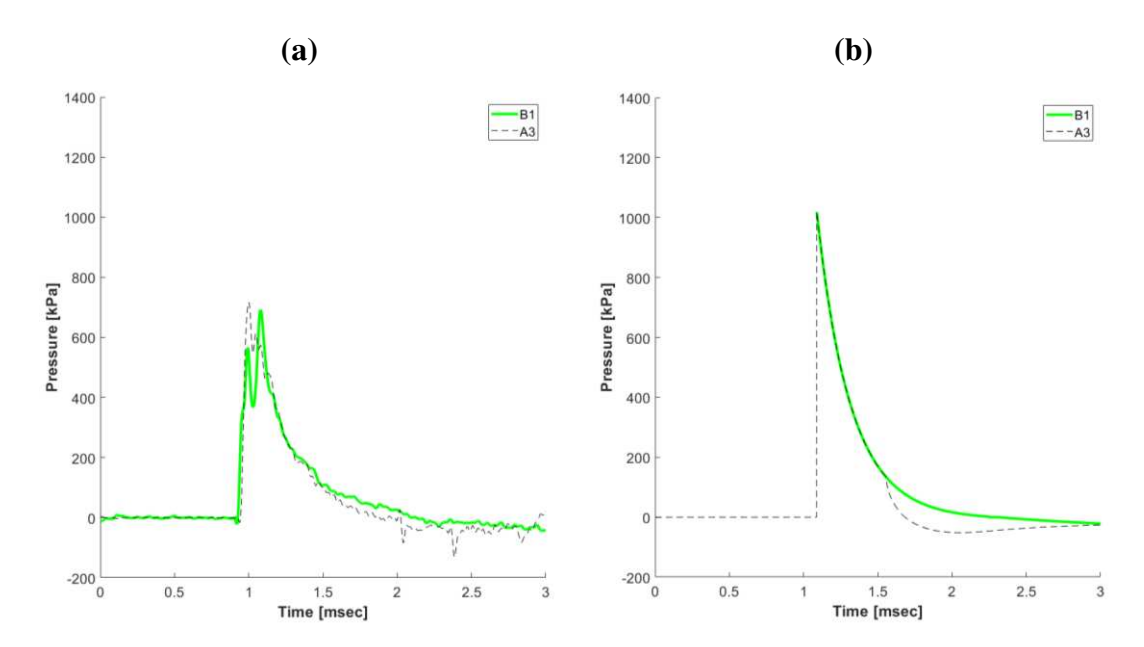


Figure 9: Assessment of clearing effects in the near-field for 170 g detonation: (a) pressure-time histories recorded from blast trials at gauges A3 and B1 in test NF_B_2, (b) pressure-time histories predicted with the Hudson method.

Figures 10 and 11 present the comparative evaluation of above-ground blast scenarios involving charge masses of 8 g and 15 g, respectively. The LAMB model exhibits strong agreement with the experimentally obtained reflected pressure-time histories on an idealised infinite surface (gauge B1). Predicted peak reflected pressures were 54 kPa and 80 kPa for the 8 g and 15 g detonations, respectively, closely matching the measured values of 58 kPa and 85 kPa. The arrival times of the incident wave were also well captured by the LAMB rules, occurring at approximately 2.3 msec and 2.1 msec for the respective charge sizes. The arrival time of the ground-reflected wave was similarly well predicted, with LAMB estimates of 3.1 msec and 2.9 msec aligning with experimental observations. However, the LAMB predictions consistently underestimated the peak amplitude of the second positive pressure. For the 8 g detonation, LAMB predicted 34 kPa (29 kPa with clearing effects), whereas experimental data indicated 43 kPa (25 kPa with clearing effects). For the 15 g charge, the model yielded 52 kPa (44 kPa with clearing effects), compared to measured values of 60 kPa (48 kPa with clearing effects). These discrepancies suggest potential limitations in the current LAMB formulation for above-ground scenarios and warrant further investigation, potentially leading to model refinements.

The Hudson method predicts the initiation of clearing due to the incident wave at 2.9 msec and 2.7 msec for the 8 g and 15 g charges, respectively. This prediction is substantiated by experimental data, which show a pressure drop at gauge A3 relative to gauge B1 at the corresponding times. These findings further validate previous CFD simulations, supporting the Hudson method's applicability in modeling clearing effects in above-ground blast environments. Regarding the clearing effects associated with the ground-reflected wave, no definitive conclusions could be drawn from the current experimental data. The Hudson method estimates the arrival of this secondary clearing wave at 4.5 msec and 4.2 msec for the respective charge masses—timing that coincides with the negative phase of the pressure-time history, where signal clarity is diminished.

Future experimental efforts will focus on configurations where the ground-reflected clearing wave intersects with the positive phase of the second pressure peak, enabling more conclusive analysis.

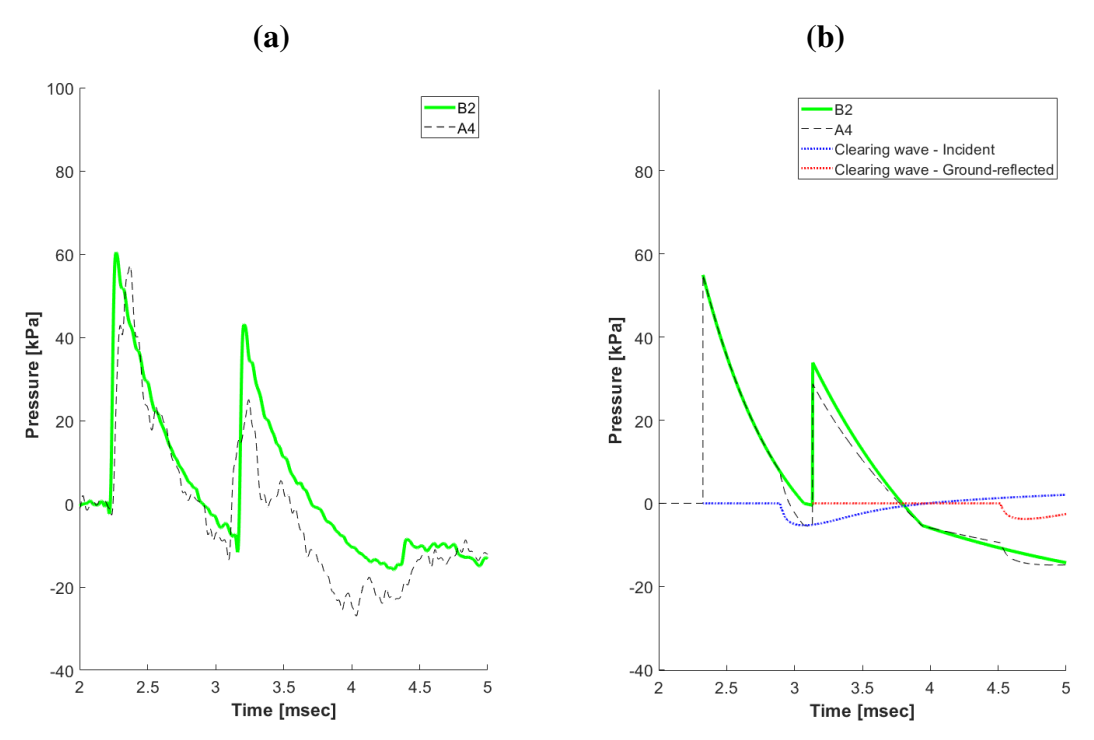


Figure 10: Assessment of clearing effects in above-ground explosions for 8 g detonation: (a) pressure-time histories recorded from blast trials at gauges A4 and B2 in test AG_A_2, (b) pressure-time histories predicted with the Hudson method.

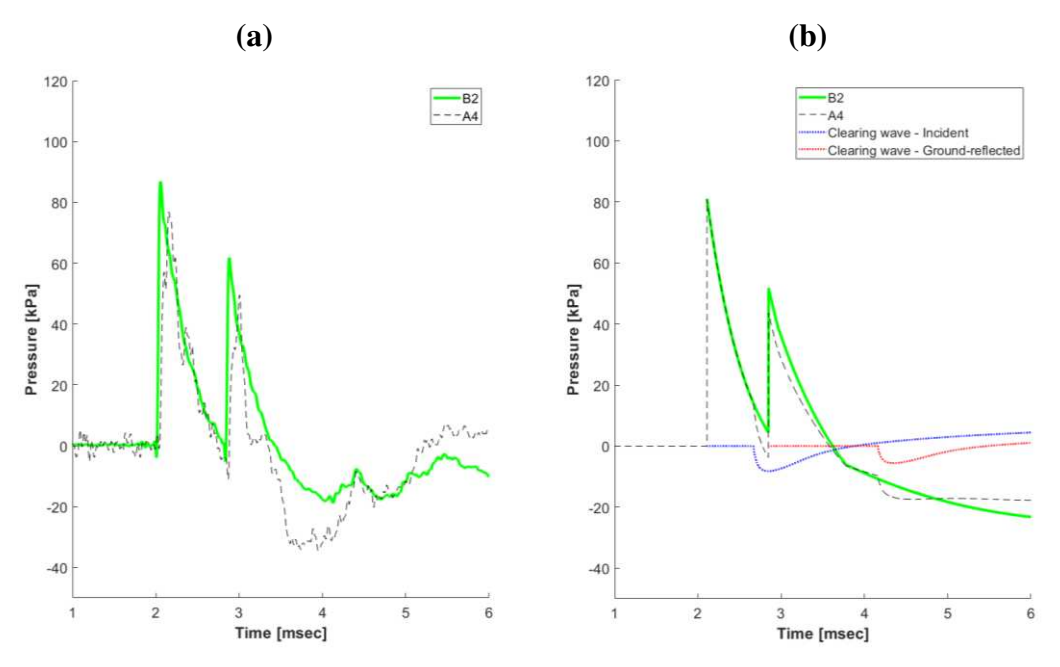


Figure 11: Assessment of clearing effects in above-ground explosions for 15 g detonation: (a) pressure-time histories recorded from blast trials at gauges A4 and B2 in test AG_B_2, (b) pressure-time histories predicted with the Hudson method.

CONCLUSIONS

This study presents a series of controlled experimental trials involving surface and above-ground explosive events, designed to investigate clearing effects and to assess the applicability of the Hudson method under varying blast conditions. Each test configuration incorporated two vertical target walls, with the charge alignment deliberately varied to produce differential boundary conditions: one wall approximated an infinite target, minimising clearing effects, while the other simulated a finite target, where clearing phenomena were expected to be more pronounced.

Surface explosion trials were conducted under near-field conditions, with scaled distances reaching as low as 2 m/kg^{1/3}. The results provide compelling empirical evidence that clearing effects remain significant even at such reduced scaled distances. Experimental data were benchmarked against predictions from the EMBlast computational tool, which integrates the Hudson method by superimposing pressure relief clearing waves—derived from Hudson's empirical graphs—onto reflected pressure-time histories generated via the semi-empirical Low Altitude Multiple Burst (LAMB) addition method. These findings corroborate prior CFD simulations, affirming the Hudson method's efficacy in modeling clearing effects in the near-field at small scaled distances.

Above-ground explosion trials revealed that clearing effects influence targets located both below and above the triple-point path. This investigation focused primarily on the later configuration, where the incident and ground-reflected waves impinge upon the target sequentially. The Hudson method was applied to these scenarios by modeling distinct pressure relief clearing waves corresponding to each wavefront. Comparative analysis between experimental measurements and EMBlast predictions further substantiated the Hudson method's validity in capturing the clearing effects associated with the initial incident wave. However, due to the temporal overlap of the ground-reflected clearing wave with the negative phase of the pressure-time history, signal fidelity was compromised, precluding definitive conclusions regarding its influence.

Future research will extend these investigations through additional near-field and above-ground trials to further elucidate clearing effects and refine the application of the Hudson method. Particular emphasis will be placed on experimental setups where the ground-reflected clearing wave intersects with the positive phase of the second pressure peak, thereby enhancing the interpretability of gauge data and enabling more rigorous validation of the method. Moreover, given indications of potential limitations in the LAMB model's ability to accurately predict the second positive peak in above-ground scenarios, further experimental scrutiny is warranted to inform potential model enhancements. Lastly, subsequent studies will aim to characterise the combined influence of angle of incidence and clearing effects on near-field pressure measurements. This will involve analysis of data from additional pressure gauges embedded in the target walls, which were not addressed in the current study, alongside expanded experimental campaigns.

ACKNOWLEDGMENTS

The authors gratefully acknowledge Innovate UK for funding this research through a Knowledge Transfer Partnership (KTP).

REFERENCES

- [1] Hudson, C. C. (1955) SC-TM-191-55-51: Sound pulse approximations to blast loading (with comments on transient drag), Sandia Corporation Technical Memorandum.
- [2] Tyas, A., Warren, J., Bennett, T., Fay, S. (2011) *Prediction of clearing effects in far-field blast loading of finite targets*, in *Shock Waves*, vol. 21, p. 111–119.
- [3] Rigby, S. E. (2014) Blast Wave Clearing Effects on Finite-Sized Targets Subjected to Explosive Loads, University of Sheffield.
- [4] Rigby, S. E., Tyas, A., Clarke, S. D., Fay, S., Reay, J. J., Warren, J., Pope, D.J. (2015) A Review of UFC-3-340-02 Blast Wave Clearing Predictions, in Proceedings of 16th International Symposium for the Interaction of the Effects of Munitions with Structures, Destin.
- [5] Nartu, M. K., Kumar, M., Ramisetti, S. B. (2022) *Improved Methodology for Accurate Prediction of Blast Wave Clearing on a Finite Target*, in *Journal of Engineering Mechanics*, vol. 148.
- [6] Angelides, S. C., Burgan, B., Kyprianou, C., Rigby, S. E., Tyas, A. (2023) An application of the Hudson clearing method to near-field blast loading and above-ground explosions, in Proceedings of the 6th International Conference on Protective Structures (ICPS6), Auburn.
- [7] Shin, J., Whittaker, A. S. (2019) *Blast-Wave Clearing for Detonations of High Explosives*, in *Journal of Structural Engineering*, vol. 145.
- [8] Rigby, S. E., Tyas, A., Clarke, S. D., Fay, S., Reay, J. J., Warren, J., Gant, M., Elgy, I. (2015) Observations from Preliminary Experiments on Spatial and Temporal Pressure Measurements from Near-Field Free Air Explosions, in International Journal of Protective Structures, vol. 6.
- [9] Angelides, S. C., Morison, C., Burgan, B., Kyprianou, C., Rigby, S. E., Tyas, A. (2023) *A methodology for predicting far-field blast loading on structures*, in *Structures*, vol. 58.
- [10] Farrimond, D. G., Woolford, S., Tyas, A., Rigby, S. E., Clarke, S. D., Clarke, S. D., Barr, A., Whittaker, M., Pope, D.J. (2023) *Far-field positive phase blast parameter characterisation of RDX and PETN based explosives*, in *International Journal of Protective Structures*, vol. 15.